



Numerical Study of the Effect of Material Type on the Properties of Photonic Crystal Fibers

Nawal N. Amsir^{1*}, Hassan A. Yasser²

Abstract

In this paper, photonic crystal fiber was designed using COMSOL environment which adopts finite element method to determine the effective refractive index. Three types of materials (SiO_2 , SF_6 , and Si_3N_4) were used for the fiber background and study the effect of air holes radius in the first ring on the properties of photonic crystal fiber. Controlling dispersion change is good in the case of silica, and the nonlinearity coefficients are higher in the case of Si_3N_4 . The model achieves two values of zero-dispersion wavelengths for all cases. The sudden changes in the nonlinearity coefficient depend on the wavelength and the type of material used.

Key Words: PCF, Dispersion, Nonlinearity Parameter.

DOI Number: 10.14704/nq.2022.20.6.NQ22250

NeuroQuantology2022;20(6):2603-2610

Introduction

Recently, photonic crystal fibers (PCFs) also known as holey fibers or micro structured optical fibers, are made up of a minute grid of air channels that form a low index cladding around an undoped silica core [1]. Have attracted interest in the fields of transmission fiber dispersion management, sensing, and telecom applications [2]. It has recently emerged as a viable contender, particularly as a dispersion compensator, because it allows us to modify dispersion qualities in ways that traditional fibers cannot. Different forms of PCF structures have already been proposed to correct for SMF dispersion [3,4].

PCF's design is extremely adaptable. Compared to standard optical fibers, photonic crystal fiber provides a number of advantages. Only a few of the advantages include single mode operation for extremely short working wavelengths, robust birefringence, tunable dispersion, single polarization single mode, maintaining single mode for large scale fiber, and regulating nonlinearity and effective mode area [5]. PCFs have outperformed its conventional step index fiber counterpart. This is due to the flexibility in the

design of the structure, the material used and application. PCFs referred to as microstructures or holey fibers have received growing interest in recent years [6].

Photonic band gap guiding and refractive index guiding, which is based on total internal reflection, are the two types of light guiding mechanisms used in PCFs. The claddings of both band gap and index guiding PCFs are made up of air holes, however the core structure differs [7]. The refractive index contrast in solid core PCFs is accomplished by the placement of air holes in the cladding. To regulate optical features such as unending single mode, high birefringence, chromatic dispersion management, big mode area, high nonlinearity, and low confinement loss, PCFs have a variety of degrees of freedom and design flexibility [8]. Nonlinear optics, sensing, high-power technologies, and telecommunications are only a few of the applications enabled by these features [9,10].

The optical qualities can be accomplished by optimizing the shape, size, and location of the air holes [11].

2603

Corresponding author: Nawal N. Amsir

Address: ^{1*}Ministry of Education, Directorate of Education in Thi-Qar; ²Physic Department, College of Science, Thi-Qar University.



E-mail: ^{1*}nawal_naj.@sci.utq.edu.iq; ²hassan.yasser@sci.utq.edu.iq

Dispersion is a measure of the optical pulse's temporal broadening and is one of the key causes of penalty for efficient optical signal transmission. In optical amplification, a PCF with strong Birefringence and negative dispersion correction is crucial because it preserves linear polarization and is beneficial for double Raman gains and sensing [12]. PCFs can be used to adjust for the positive dispersion parameter and dispersion slope with success. Additionally, near the communication wavelength, they can be made to exhibit ultranegative dispersion values [13].

The main objective of this paper is to analyze physical properties of the PCF to control dispersion and nonlinearity for different materials and different values of structural parameters varied over a wide range of wavelength.

Model Design

The proposed PCF consists of four rings of air holes, the central region (the core) is solid and the cladding is perforated. The first ring with a radius of d_1 , and in it there are twelve holes with radii of a_1 placed at the angles $\theta_1 = n\pi/6, n = 0, 1, 2, \dots$. The second ring with a radius of d_2 , that contains fourteen holes with radii of a_2 placed at the angles $\theta_2 = n\pi/7, n = 0, 1, 2, \dots$. The third ring with a radius of d_3 has sixteen holes with radii of a_3 placed at the angles $\theta_3 = n\pi/8, n = 0, 1, 2, \dots$. Also, the fourth ring has radius d_4 , and in it there are sixteen holes with radii of a_4 placed at the angles $\theta_4 = n\pi/8, n = 0, 1, 2, \dots$. The fiber background is composed of one material to be selected from the materials: $\text{SiO}_2, \text{SF}_6, \text{and } \text{Si}_3\text{N}_4$.

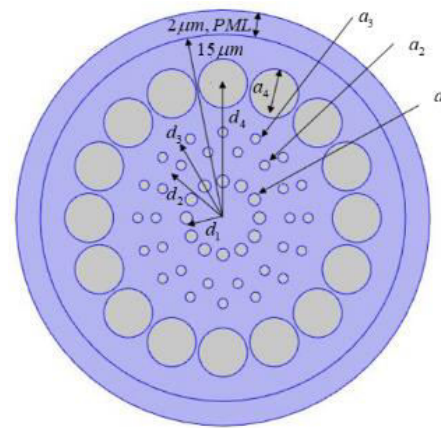
Finally, the fiber is surrounded by an perfect matched layer (PML) in order to prevent scattering and reflections through the fiber region. Fig.(1a) obtains the cross section of the proposed model, while table(1) represents the parameter value of the proposed PCF. The wave equation through the PCF is solved to calculate the effective refractive index, where we adopt the finding of the fundamental mode for this purpose. Fig.(1b) illustrates the fundamental mode in the solid core region.

Theoretical Formalism

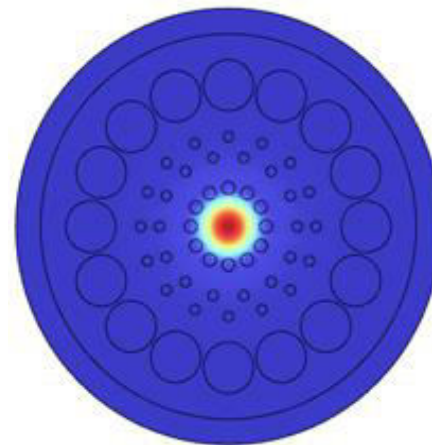
The refractive index (RI) within certain ranges of wavelengths of employed background ($\text{SiO}_2, \text{SF}_6, \text{Si}_3\text{N}_4$) are varied by Sellmeier's equation as follows [14]

$$n(\lambda) = \sqrt{1 + \sum_{j=1}^m \frac{A_j \lambda^2}{\lambda^2 - B_j}} \quad (1)$$

where λ is the wavelength of light in (μm) and the Sellmeier's coefficients A'_s, B'_s are shown in table(2).



(a)



(b)

Fig.1. a) the proposed PCF design and b) the fundamental mode, where the fiber background is composed from one the materials $\text{SiO}_2, \text{SF}_6, \text{Si}_3\text{N}_4$ and the holes are air

Table2.Parameters of the suggested PCF

parameter	value	parameter	value
PCF radius	$15 \mu\text{m}$	d_1	$3 \mu\text{m}$
a_1	$(0.2, 0.3, 0.4) \mu\text{m}$	d_2	$5.5 \mu\text{m}$
a_2	$0.2 \mu\text{m}$	d_3	$7 \mu\text{m}$



a_3	$0.2\mu m$	d_4	$11\mu m$
a_4	$2\mu m$	PML thickness	$2\mu m$

The amplitude of an electromagnetic wave changes as it propagates in a particular direction, and the propagation constant is a measure of that change. The effective refractive index is related to the propagation constant as $n_{eff} = \beta / k_o$ where $k_o = 2\pi / \lambda$ is the propagation constant in vacuum. The propagation constant can be mathematically expressed as a Taylor series around w_o as [15]

$$\beta(w) = \beta_o + \beta_1(w - w_o) + \frac{1}{2}\beta_2(w - w_o)^2 + \frac{1}{6}\beta_3(w - w_o)^3 + \dots \quad (2)$$

where $\beta_m = (d\beta / dw)_{w=w_o}$. The parameters β_1 and β_2 (they are responsible for group velocity and group velocity dispersion, respectively) are related to the refractive index $n(\omega)$ and its derivatives through the relations

$$\beta_1 = \frac{d\beta_o}{dw} = -\frac{1}{c} \left[n_{eff} - \lambda \frac{dn_{eff}}{d\lambda} \right] \quad (3a)$$

$$\beta_2 = \frac{d\beta_1}{dw} = -\frac{\lambda^3}{2\pi c^2} \frac{d^2 n_{eff}}{d\lambda^2} \quad (3b)$$

Here, the parameters $\beta_n, n = 2, 3, 4, \dots$. The parameter β_n is responsible for the nth order of group velocity dispersion.

Dispersion is a significant element that limits the amount of data that a fiber cable can carry. The presence of dispersion causes the pulse to propagate, resulting in intersymbol interference. It is divided into two types: Dispersions on both the intermodal and intramod. The first type is seen in multimode fiber. In single-mode fibers, the second type, often known as chromatic dispersion, is critical. The chromatic dispersion is a combination of material and waveguide dispersions [20].

For optical communications, dispersion compensation, and nonlinear applications, PCF dispersion is a critical issue. The radius of holes, the radius of rings, the number of rings, and the distances between rings holes may all be changed to regulate the dispersion property of PCF. The link between the effective refractive index, and the wavelength can be found by solving the wave equation. As a result, we estimated the structure's second order chromatic dispersion as [21]

$$D = -\frac{2\pi c}{\lambda^2} \beta_2 = -\frac{\lambda}{c} \frac{d^2 Re\{n_{eff}\}}{d\lambda^2} \quad (5)$$

Here Re refers to the real part of the effective index obtained from the simulation and c is the velocity of light in vacuum.

This PCF was designed using proper design parameters using COMSOL Multiphysics, which is based on FEM and PML conditions. The cross section of this PCF is divided into subspaces, and Maxwell equations are solved by finding the adjacent subspaces in order to establish its optical properties. The effective refractive index is determined by utilizing FEM to solve the eigenvalue issue derived from Maxwell's equations. [22]

$$\vec{\nabla} \times ([s^{-1} \vec{\nabla} \times \vec{E}]) - k_o^2 n^2 [s] \vec{E} = 0 \quad (6)$$

where \vec{E} is the electric field vector, $[s]$ is the PML matrix, $[s^{-1}]$ is the inverse matrix of $[s]$, n is the refractive index of the domain.

Nonlinear coefficient is one of the most important parameters and has been defined as [23]

$$\gamma = \frac{2\pi n_2}{\lambda A_{eff}} \quad (7)$$

where A_{eff} is the effective area that provides a measure of the area covered effectively by a mode inside the fiber and n_2 is the nonlinear refractive

Table1. Parameters of the selected media [16,17,18,19]

material parameters	SCHOTT glass SF ₆	SiO ₂	Si ₃ N ₄
A_1	1.72448482	0.6961663	3.0249
A_2	0.390104889	0.4079426	40314
A_3	1.04572858	0.8974794	-
$B_1(\mu m^2)$	0.013487195	0.0046791483	0.018317078
$B_2(\mu m^2)$	0.05693181	0.0135120631	1537208.19
$B_3(\mu m^2)$	118.557185	97.934002538	-
$n_2(m^2/W)$	2.1×10^{-19}	2.6×10^{-20}	1.4×10^{-18}
Range of $\lambda(\mu m)$	0.365 - 2.5	0.21 - 6.7	0.31- 5.504

In general, we obtain the following equation to determine the higher order dispersion parameters

$$\beta_n = \frac{d\beta_{n-1}}{dw} = -\frac{\lambda^2}{2\pi c} \frac{d\beta_{n-1}}{d\lambda} \quad n = 3, 4, \dots (4)$$



indices of the material, as in table(2) for the present materials. The parameter A_{eff} is given by [23]

$$A_{eff} = \frac{\left[\int_{-\infty}^{\infty} \int_{-\infty}^{\infty} |E(x, y)|^2 dx dy \right]^2}{\int_{-\infty}^{\infty} \int_{-\infty}^{\infty} |E(x, y)|^4 dx dy} \quad (8)$$

where E is the magnitude of electric field component that will be determined by solving an eigen value problem drawn from Maxwell's equations.

Results and Discussion

Fig.(2) shows the effective refractive index as a function of wavelength using three fiber background materials and three values of a_1 . It appears from the figure that silica has a semi-linear relationship and the appearance of curvature in the curves of other materials. A change of a_1 causes a slight change in the case of silica and a smaller change in the other materials. In general, the curves decrease with an increase in a_1 for all cases, and

this is physically acceptable, since an increase in a_1 means an increase in the proportion of air in the section of the fiber.

Fig.(3) represents the effective area of the pattern using the three materials as a background material for the fiber and adopting three values of a_1 . In the case of $a_1 = 0.2 \mu m$, the relationship is gradually increasing for all materials, in case $a_1 = 0.3 \mu m$ it remains gradually increasing for the two materials SF_6, Si_3N_4 and increases dramatically at the wavelength $\lambda = 1.5 \mu m$ for the silica material. In the case $a_1 = 0.4 \mu m$, only the gradual increase remains for material Si_3N_4 , and sudden increases occur in the case of the other two materials at wavelengths $1.3 \mu m, 1.8 \mu m$, respectively. The above behaviors of the spot of the fundamental mode are caused by the relationship between the refractive indices of materials and air at different wavelengths, as the material Si_3N_4 did not undergo sudden changes because it has the largest refractive index. Generally, before sudden changes occur, a smaller value of a_1 gives a larger spot size for different wavelengths.

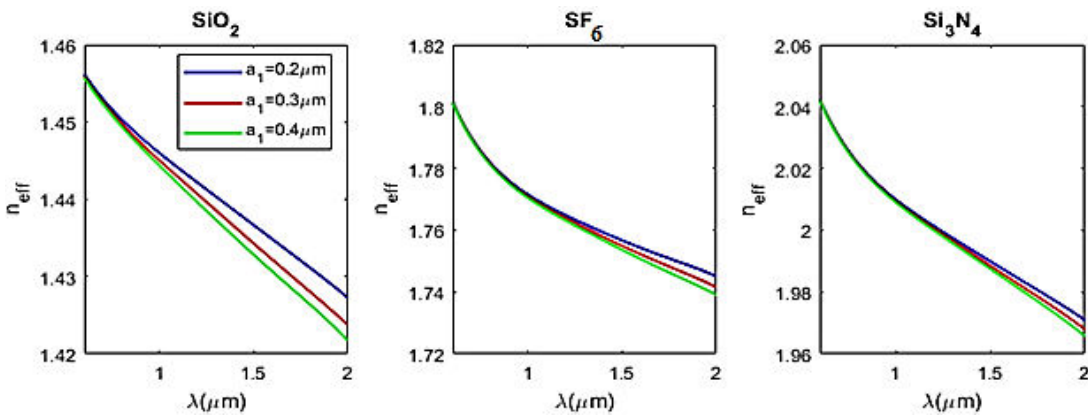


Fig.2. The effective refractive index as a function of wavelength using different materials for $a_1 = (0.2, 0.3, 0.4) \mu m$

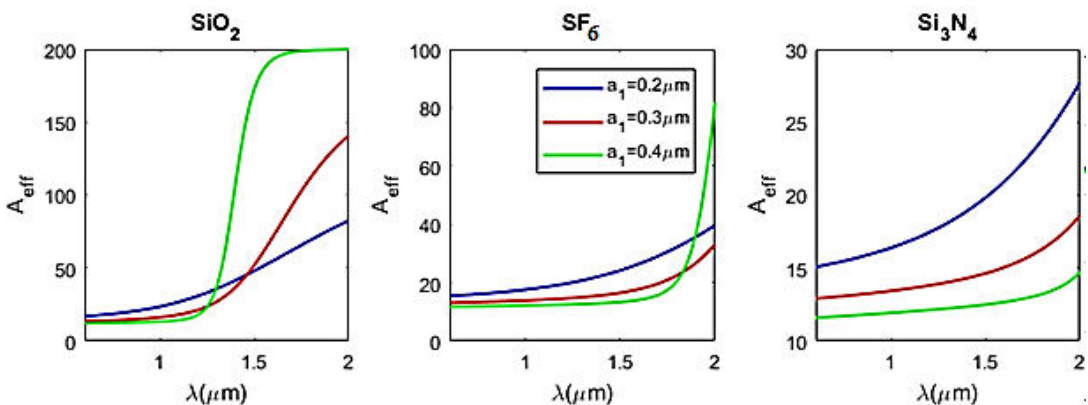


Fig.3. The effective mode area as a function of wavelength using different materials for $a_1 = (0.2, 0.3, 0.4) \mu\text{m}$

For all cases, the effective area is as large as possible for material SF_6 and least for silica. Since the coefficient of nonlinearity is inversely proportional to the effective area, Fig.(4) shows the gradual decreasing of the coefficient of nonlinearity with the increase in wavelength and the sudden

changes that we referred to above at some wavelengths. The largest values of nonlinearity are obtained using material Si_3N_4 and the lowest for silica for all cases. A high nonlinearity parameter is useful in many applications.

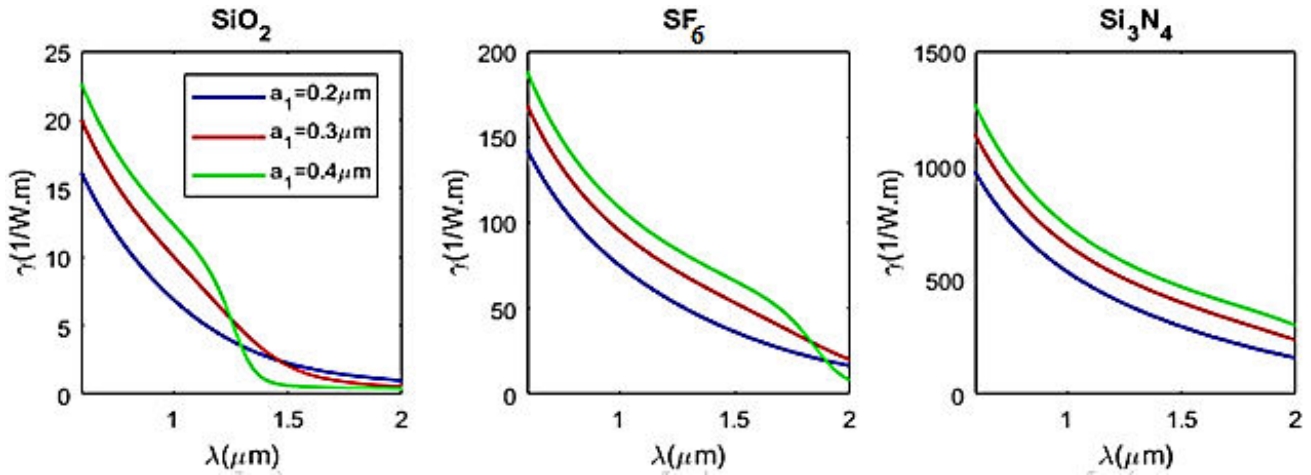


Fig.4. The nonlinearity parameter as a function of wavelength using different materials for $a_1 = (0.2, 0.3, 0.4) \mu\text{m}$

Fig.(5) and (6) obtain the dispersion and second order GVD as functions of wavelength using three fiber background materials and three values of a_1 . All cases have two point of zero dispersion wavelength around $\lambda = 1.5 \mu\text{m}$. Therefore, all cases achieve an anomalous dispersion regime ($D > 0, \beta_2 < 0$) around $\lambda = 1.5 \mu\text{m}$ and a normal dispersion regime ($D < 0, \beta_2 > 0$) for

other wavelengths. The wavelength range that achieves an anomalous dispersion regime varies from one material to another and varies according to the values of a_1 . Changing a_1 will cause a large change in the dispersion curve for silica, but changing it for other materials does not cause significant changes. The zero-dispersion wavelengths are useful in optical communications and other applications.

2607

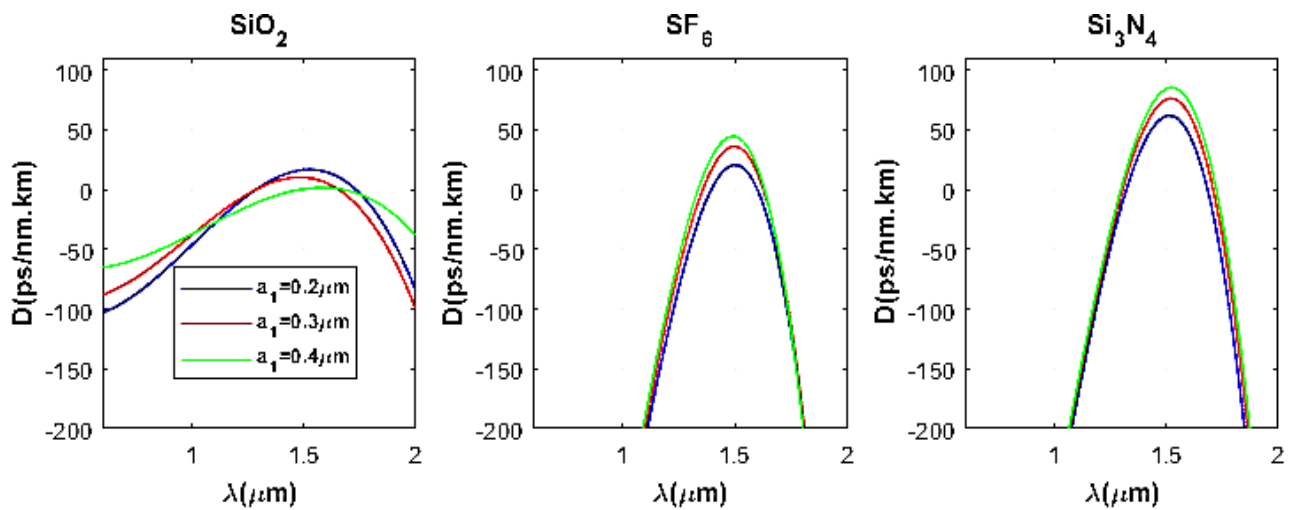


Fig.5. The dispersion as a function of wavelength using different materials for $a_1 = (0.2, 0.3, 0.4) \mu\text{m}$



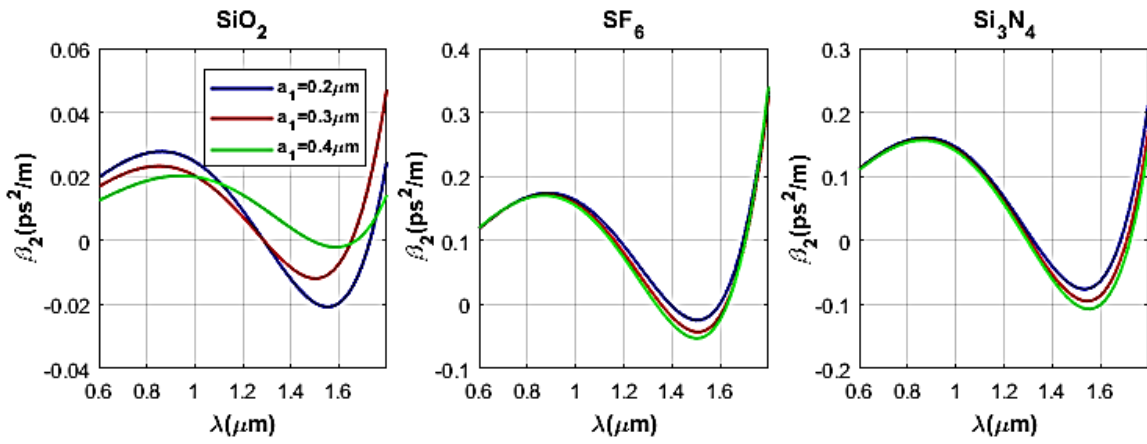


Fig.6. The second order GVD as a function of wavelength using different materials for $a_1 = (0.2, 0.3, 0.4) \mu\text{m}$

Figs.(7) to (9) explain the third, fourth and fifth orders of GVD as functions of wavelength using three fiber background materials and three values of a_1 . Change a_1 causes large changes in $\beta_3, \beta_4, \beta_5$ values for silica and small changes for other materials. In general, changing the type of

material causes a large change in the curves. There are one or two wavelengths in which the coefficients $\beta_3, \beta_4, \beta_5$ are zero. We can deduce higher orders GVD which are important in the supercontinuum generation phenomenon.

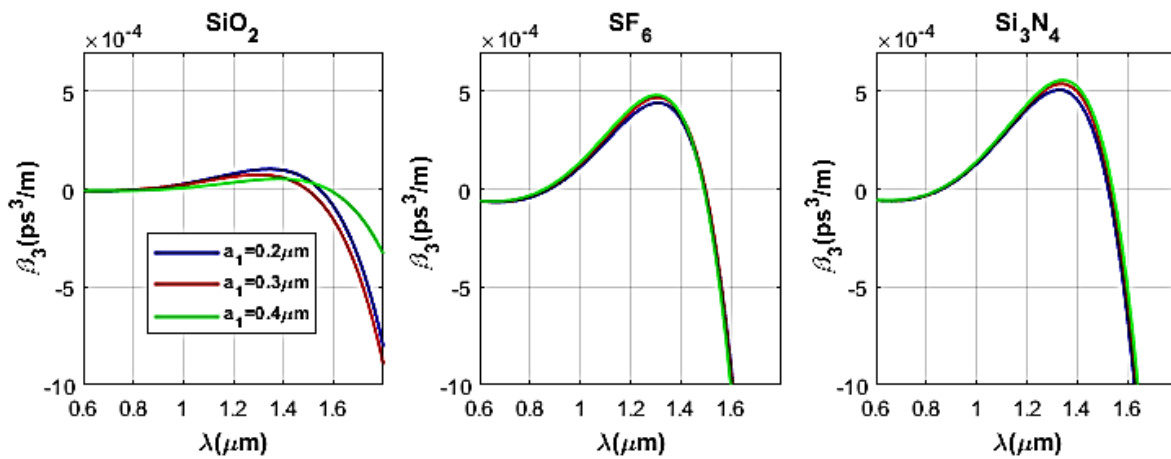


Fig.7. The third order GVD as a function of wavelength using different materials for $a_1 = (0.2, 0.3, 0.4) \mu\text{m}$

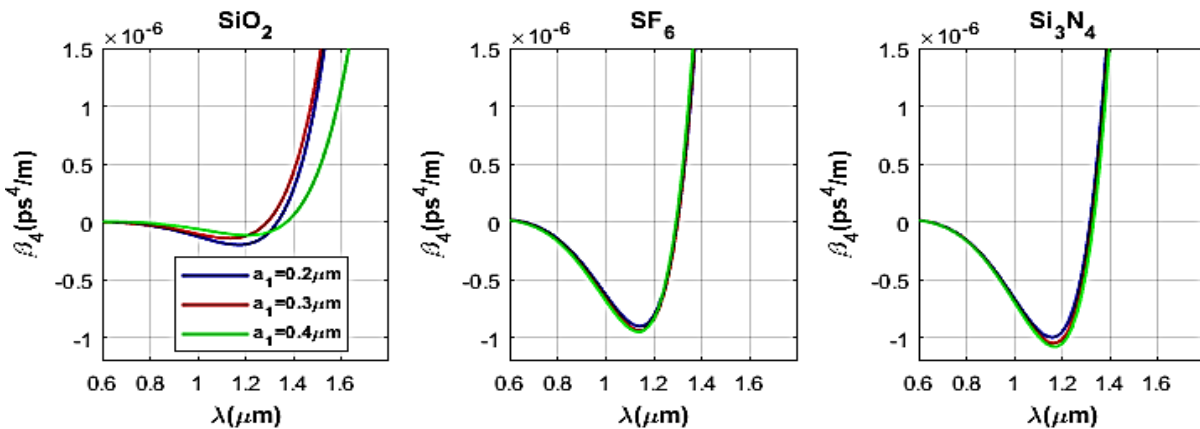


Fig.8. The fourth order GVD as a function of wavelength using different materials for $a_1 = (0.2, 0.3, 0.4) \mu\text{m}$



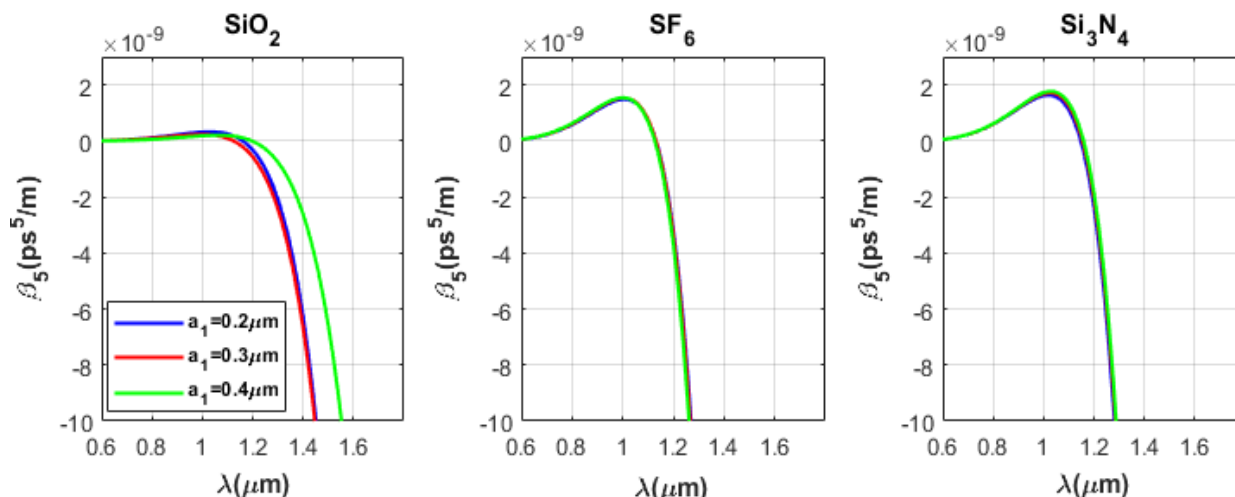


Fig.9. The fifth order GVD as a function of wavelength using different materials for $a_1 = (0.2, 0.3, 0.4) \mu\text{m}$

Conclusions

As a conclusion, different materials exhibit different nonlinearity and dispersion properties. The type of material used and the wavelength may cause sudden changes in the nonlinearity of the two materials SiO_2 and SF_6 . The achieved dispersion depends strongly on a_1 especially for silica. The diversity of dispersion achieved in silica material is the best. For all GVD orders, silica shows obvious changes due to a_1 value. Controlling the type of material and the a_1 enables us to realize an anomalous or normal regime.

References

- M. Haque, M. Rahman, M. Habib, M. Habib, and S. Razzak, "A new circular photonic crystal fiber for effective dispersion compensation over E to L wavelength bands", *Journal of Microwaves, Optoelectronics and Electromagnetic Applications*, 12(2), 281-291, 2013.
- S. Varshney, T. Fujisawa, K. Saitoh, and M. Koshiba, "Design and analysis of a broadband dispersion compensating photonic crystal fiber Raman amplifier operating in S-band", *Opt. Express*, vol. 14, no. 8, pp. 3528-3540, 2006.
- F. Begum, Y. Namihira, S. Razzak, S. Kaijage, N. Hai, T. Kinjo, K. Miyagi, and N. Zou, "Novel broadband dispersion compensating photonic crystal fibers: Applications in high speed transmission", *Opt. Laser Technol.*, 41(6), 679-686, 2009.
- F. Gerome, J. Auguste, S. Fevrier, J. Maury, J.M. Blondy, and L. Gasca, "Dual concentric core dispersion compensating fiber optimized for WDM application", *Electron Lett.*, 41(3), pp. 116-117, 2005.
- R. Buczynski, "Photonic crystal fibers", *Acta Physica Polonica Series A*, 106(2), 141-168, 2004.
- P. Agbemabiese, and E. Akowuah, "Numerical analysis of photonic crystal fiber of ultra-high birefringence and high nonlinearity", *Scientific Reports*, 10(1), 1-12, 2020.
- K. Saitoh, and M. Koshiba, "Leakage loss and group velocity dispersion in air-core photonic bandgap fibers", *Opt. Express* 11, 3100-3109, 2003.
- M. Chen, and S. Xie, "New nonlinear and dispersion flattened photonic crystal fiber with low confinement loss", *Opt. Commun.* 281, 2073-2076, 2008.
- G. Agrawal, "Nonlinear fiber optics: its history and recent progress". *JOSA B* 28, A1-A10, 2011.
- J. Limpert, T. Schreiber, S. Nolte, H. Zellmer, A. Tunnermann, R. Iliew, F. Lederer, J. Broeng, G. Vienne, A. Petersson, and C. Jakobsen, "High-power air-clad large-mode-area photonic crystal fiber laser", *Opt. Express* 11, 818-823, 2003.
- S. Verma, "All-circular hole microstructured fiber with high birefringence and low confinement loss", *Appl. Opt.* 58, 3767-3774, 2019.
- Y. Lee, C. Lee, Y. Jung, M. Oh, and S. Kim, "Highly birefringent and dispersion compensating photonic crystal fiber based on double line defect core", *J. Opt. Soc. Korea* 20, 567-574, 2016.
- A. Bouk, A. Cucinotta, F. Poli, and S. Selleri, "Dispersion properties of square-lattice photonic crystal fibers", *Optics Express*, vol. 12, no. 5, pp. 941-946, 2004.
- A. Talib, and H. Yasser, "Maximizing spectral sensitivity of plasmonic photonic crystal fiber sensor", *Optik*, 249, 168228, 2022.
- J. Epping, "Dispersion engineering silicon nitride waveguides for broadband nonlinear frequency conversion". University of Twente, 2015.
- www. Refractive index information
- V. Kalashnikov, E. Sorokin, and I. Sorokina, "Raman effects in the infrared supercontinuum generation in soft-glass PCFs", *Applied Physics B*, 87(1), 37-44, 2007.
- H. Mbonde, H. Frankis, and D. Bradley, "Enhanced nonlinearity and engineered anomalous dispersion in TeO_2 -coated Si_3N_4 waveguides", *IEEE Photonics Journal*, 12(2), 1-10, 2020.
- M. Ferhat, L. Cherbi, and I. Haddouche, "Supercontinuum generation in silica photonic crystal fiber at 1.5 μm and 1.65 μm wavelengths for optical coherence tomography", *Optik*, vol. 152, 106-115, 2018.



- L. Tévenaz, "Advanced fiber optics",EPFL Press, Lausanne, 2011.
- A. Bouk, A. Cucinotta, F. Poli, and S. Selleri, "Dispersion properties of square-lattice photonic crystal fibers", Optics Express, vol. 12, no. 5, pp. 941-946, 2004.
- S. Asaduzzaman, K. Ahmed, T. Bhuiyan, andT. Farah, "Hybrid photonic crystal fiber in chemical sensing",SpringerPlus, 5(1), 1-11,2016.
- N. Mohammad, and S. Al-Bassam,"Design and Characterization Study of Endless Single Mode (ESM) Photonic Crystal Fiber Using Finite Element Method",International Journalof Innovative Research in Science Engineering and Technology,vol.5,16314-16320,2016.

